11

The Uses of Artificial Intelligence for Electric Vehicle Control Applications

Brahim Gasbaoui and Abdelfatah Nasri
Bechar University, Faculty of Sciences and Technology,
Department of Electrical Engineering,
Algeria

1. Introduction

This chapter presents a novel speed control design of electric vehicle (EV) to improve the comportment and stability under different road constraints condition. The control circuit using intelligent fuzzy PI controller is proposed. Parameters which guide the functioning of PI controller are dynamically adjusted with the assistance of fuzzy intelligent control. Actually, electric vehicle (EV) including, full cell and hybrid vehicle have been developed very rapidly as a solution to energy and environmental problem. Driven EVs are powered by electric motors through transmission and differential gears, while directly driven vehicles are propelled by in-wheel or, simply, wheel motors [1, 2]. The basic vehicle configurations of this research has two directly driven wheel motors installed and operated inside the driving wheels on a pure EV. These wheel motors can be controlled independently and have so quick and accurate response to the command that the vehicle chassis control or motion control becomes more stable and robust, compared to indirectly driven EVs. Like most research on the torque distribution control of wheel motor, wheel motors [3, 15] proposed a dynamic optimal tractive force distribution control for an EV driven by four wheel motors, thereby improving vehicle handling and stability [4, 5].

Research has shown that EV control methods such as, PI control are able to perform optimally over the full range of operation conditions and disturbances and it is very effective with constant vehicle torque, Moreover these non-linear vehicle torque are not fixed and change randomly. However EV with conventional PI control may not have satisfactory performance in such fast varying conditions, the system performance deteriorates. In addition to this, it is difficult to select suitable control parameters K_p and Ki in order to achieve satisfactory compensation results while maintaining the stability of EV traction, due to the highly complex, non-linear nature of controlled systems. These are two of the major drawbacks of the PI control. In order to overcome these difficulties, adaptive PI controller by fuzzy control has been applied both in stationary and under roads constraints, and is shown to improve the overall performance of EV.The Direct Torque Control strategy (DTC) is one kind of high performance driving technologies for AC motors, due to its simple structure and ability to achieve fast response of flux and torque has attracted growing interest in the recent years. DTC-SVM with PI controller direct torque control without hysteresis band can effectively reduce the torque ripple, but its system's robustness will be fur there enhanced. DTC-SVM

method can improve the system robustness, evidently reduce the torque and flux ripple, and effectively improve the dynamical performance. The DC-DC converter is use with a control strategy to assure the energy require for the EV and the propulsion system. The aim of this chapter is to contribute to understanding the intelligent fuzzy PI controller for utility EV tow rear deriving wheel applied direct torque control based space vector modulation under several scenarios.

2. Electric vehicle description

According to Fig. 1 the opposition forces acting to the vehicle motion are: the rolling resistance force F_{tire} due to the friction of the vehicle tires on the road; the aerodynamic drag force F_{aero} caused by the friction on the body moving through the air ; and the climbing force F_{slope} that depends on the road slope [1,2 3].

The total resistive force is equal to F_r and is the sum of the resistance forces, as in (1).

$$F_r=F_{tire}+F_{aero}+F_{slope} \tag{1}$$

The rolling resistance force is defined by:

$$F_{tire}=mgf_r \tag{2}$$

The aerodynamic resistance torque is defined as follows:

$$F_{aero}=1/2\ \rho_{air}A_fC_dv^2 \tag{3}$$

The rolling resistance force is usually modeled as:

$$F_{slope}=mgsin(\alpha) \tag{4}$$

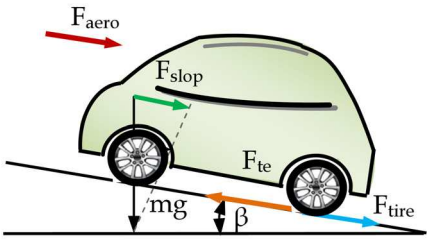

Fig. 1. The forces acting on a vehicle moving along a slope.

Where M_v is the total masse of vehicle r is the tire radius, f_r is the rolling resistance force constant, g the gravity acceleration, ρ_{AIR} is Air density , C_d is the aerodynamic drag coefficient,A_f is the frontal surface area of the vehicle, v is the vehicle speed, is the road slope angle. Values for these parameters are shown in Table1.

r	0.32 m	A_f	2.60 m^2
m	1300 Kg	C_d	0.32
f_r	0.01	ρ_{air}	1.2 Kg/m^3

Table 1. Parameters of the electric vehicle model

3. Direct torque control strategy based space vector modulation (SVM-DTC)

With the development of microprocessors and DSP techniques, the SVM technique has become one of the most important PWM methods for Voltage Source Inverter (VSI) since it gives a large linear control range, less harmonic distortion, fast transient response, and simple digital implementation. The induction motor stator flux can be estimated by:

$$\varphi_{qs} = \int_0^t (V_{qs} - R_s i_{qs})dt \tag{5}$$

$$|\varphi_s| = \sqrt{\varphi_{ds}^2 + \varphi_{qs}^2} \tag{6}$$

$$\varphi_s = \tan^{-1}\left(\frac{\varphi_{qs}}{\varphi_{ds}}\right) \tag{7}$$

And electromagnetic torque T_{em} can be calculated by:

$$T_{em} = \frac{3}{2} p(\varphi_{ds} i_{qs} - \varphi_{qs} i_{ds}) \tag{8}$$

The SVM principle is based on the switching between two adjacent active vectors and two zero vectors during one switching period. It uses the space vector concept to compute the duty cycle of the switches.

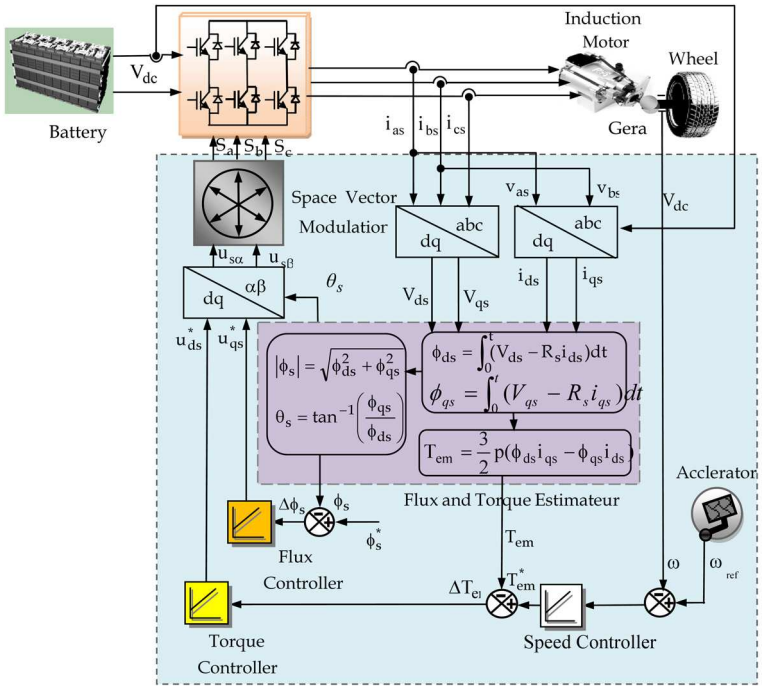

Fig. 2. Bloc diagram for DTC strategy based space vector modulation

4. Conventional PI controller

The reason behind the extensive use of proportional integral (PI) ..controller is its effectiveness in the control of steady-state error of a control system and also its easy implementation. However, one disadvantage of this conventional compensator is its inability to improve the transient response of the system. The conventional PI controller figure 3 has the form of Eq. (9), where T_{em}^{*} is the control output. Kp and Ki are the proportional and integral gains respectively, these gains depend on the system parameters. ε is the error signal, which is the difference of the injected voltage to the reference voltage.

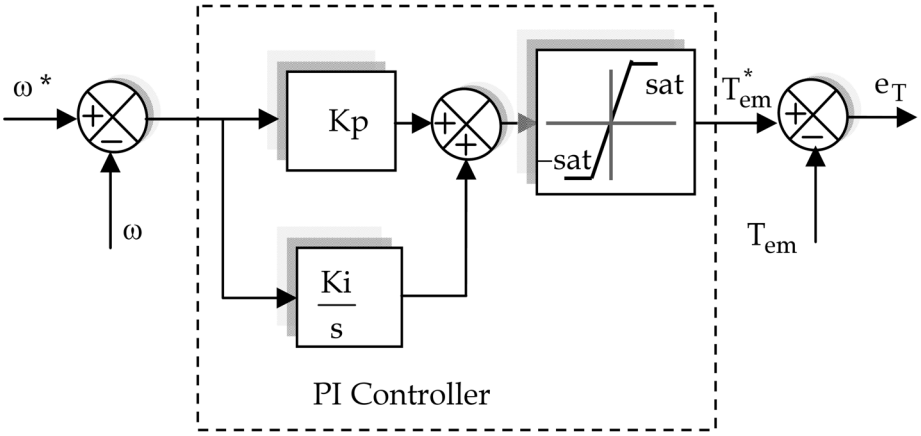

Fig. 3. Control of the injected speed using conventional PI controller

$$T_{em}(t) = Kp\varepsilon(t) + Ki\int_{T}\varepsilon(t)dt \tag{9}$$

Equation (9) shows that the PI controller introduces a pole in the entire feedback system, consequently, making a change in its original root locus. Analytically the pole introduces a change in the control system's response. The effect is the reduction of steady-state error. On the other hand, the constants Kp and Ki determine the stability and transient response of the system, in which, these constants rely on their universe of discourses: $Kp \in [Kp_{\min}, Kp_{\max}] and \quad Ki \in [Ki_{\min}, Ki_{\max}]$

Where the values of the minimum and maximum proportional and integral constants (gains) are practically evaluated through experimentation and using some iterative techniques. This makes the design of the conventional PI controller dependent on the knowledge of the expert. When the compensator constants exceed the allowable values, the control system may come into an unstable state. After the determination of the domain of the proportional and integral constants, the tuning of the instantaneous values of the constants takes place. Depending on the value of the error signal, ε, the values of the constants adjusts formulating an adaptive control system. The constants Kp and Ki changes to ensure that the steady-state error of the system is reduced to minimum if not zero.

5. Adaptive fuzzy PI controller

Fuzzy controllers have been widely applied to industrial process. Especially, fuzzy controllers are effective techniques when either the mathematical model of the system is nonlinear or not the mathematical model exists. In this paper, the fuzzy control system adjusts the parameter of the PI control by the fuzzy rule. Dependent on the state of the system . The adaptive PI realized is no more a linear regulator according to this principle. In most of these studies, the Fuzzy controller used to drive the PI is defined by the authors from a series of experiments [21, 22, 23, 24].

The expression of the PI is given in the equation (10).

$$y(t) = Kp * [e(t) + \frac{1}{T_i}\int_0^t e(t)dt] \tag{10}$$

Where:

$y(t)$: Output of the control.

$e(t)$: Input of the control. The error of the reference current $w^*(t)$ and the injected speed $w(t)$

kp: Parameter of the scale

Ti: Parameter of the integrator.

The discrete equation:

$$y(k) = Kp * [e(k) + \frac{1}{T_i}\sum_{j=1}^{k} e(j)T] \tag{11}$$

Where:

$y(k)$: Output on the time of k th sampling.

$e(k)$: Error on the time of k sampling

T : Cycle of the sampling

$$\Delta e(k) = e(k) - e(k-1)$$

$$y(k) = Kp * [e(t) + \frac{1}{T_i}\sum_{j=1}^{k} e(j)T]$$

$$y(k) = Kp * e(t) + K_i \sum_{j=1}^{k} e(j)$$

On-line Tuning:

The on-line tuning equation for kp and ki are show above:

$$kp = 20 + 0.8(Kp - 2.5) \tag{12}$$

$$ki = 0.0125 + 0.003(Ki - 2.5) \tag{13}$$

The frame of the fuzzy adaptive PI controller is illustrated in figure 4.

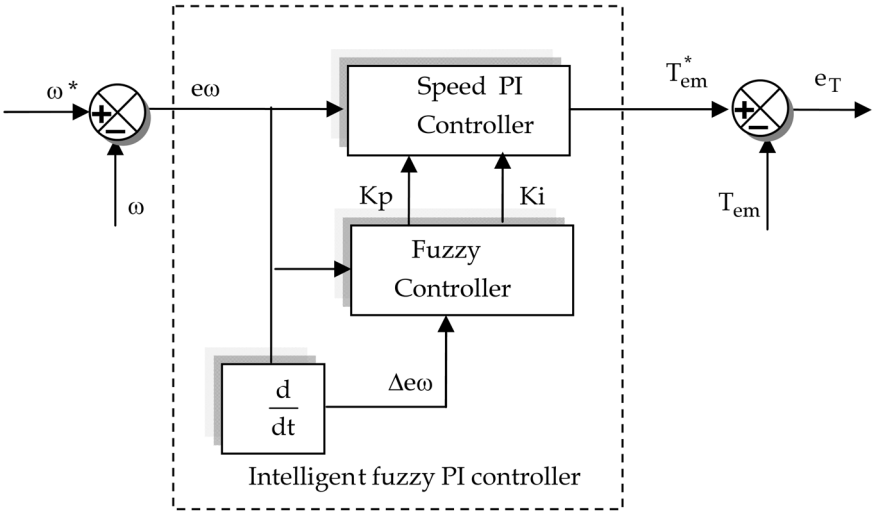

Fig. 4. PI gains online tuning by fuzzy logic controller

The linguistic variables are defines as {NL,NM,NS,Z,PS,PM,PB}meaning negative large, negative medium ,negative small, zero, positive small, positive medium, positive big.

The Membership function is illustrated in the figures 7, 8, 9 and 10.Figures 9 and 10 shows the view plot of fuzzy controller for kp and ki respectively.

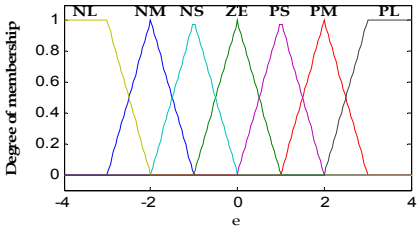

Fig. 5. The Membership function of input e(k).

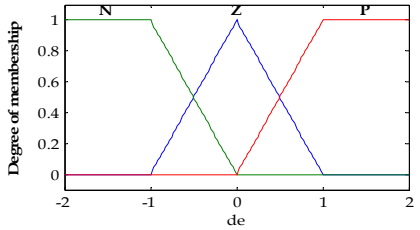

Fig. 6. The Membership function of input $\Delta e(k)$.

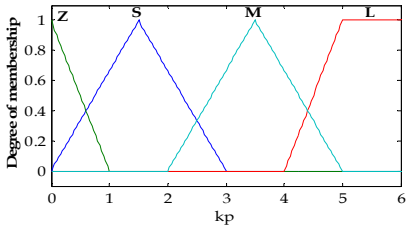

Fig. 7. The Membership functions of output kp.

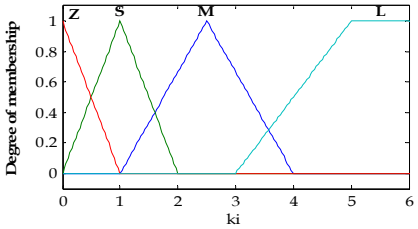

Fig. 8. The Membership function of output ki.

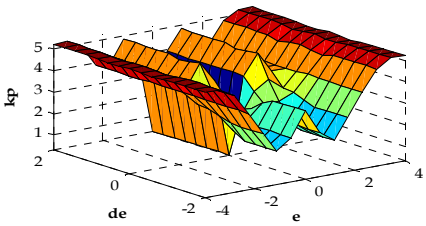

Fig. 9. View plot surface of fuzzy controller for kp

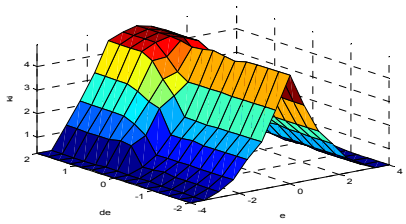

Fig. 10. View plot surface of fuzzy controller for ki

kp and ki	$\Delta e(\omega)$ \ $e(\omega)$	NL	NM	NS	ZE	PS	PM	PB
kp	N	L	M	S	M	S	M	L
	Z	L	M	L	Z	L	M	L
	P	L	M	L	Z	L	M	L
ki	N	Z	S	M	L	M	S	Z
	Z	Z	S	M	L	M	S	Z
	P	Z	M	L	L	L	M	Z

Table 2. Fuzzy tuning rules

6. Implementation of electronic differential

The proposed control system principle could be summarized as follows:

A speed control is used to control each motor torque. The speed of each rear wheel is controlled using speed difference feedback. Since the two rear wheels are directly driven by two separate motors, the speed of the outer wheel will need to be higher than the speed of the inner wheel during steering maneuvers (and vice-versa). This condition can be easily met if the speed estimator is used to sense the angular speed of the steering wheel. The common reference speed ω_{ref} is then set by the accelerator pedal command. The actual reference speed for the left drive ω^*_{left} and the right drive ω^*_{right} are then obtained by adjusting the common reference speed ω^* using the output signal from the DTC speed estimator. If the vehicle is turning right, the left wheel speed is increased and the right wheel speed remains equal to the common reference speed ω^*. If the vehicle is turning left, the right wheel speed is increased and the left wheel speed remains equal to the common reference speed ω^* [7, 9, and 11]. Usually, a driving trajectory is adequate for an analysis of the vehicle system model. From the mode show in Fig. 6, the following characteristic can be calculated:

$$R_\omega = \frac{L_\omega}{tg(\delta)} \tag{14}$$

Where δ is the steering angle. Therefore, the linear speed of each wheel drive is given by:

$$\begin{cases} V_1 = \omega_v (R - d_\omega / 2 \\ V_2 = \omega_v (R - d_\omega / 2 \end{cases} \tag{15}$$

And their angular speed by:

$$\begin{cases} V_1 = \omega_v (R - d_\omega / 2 \\ V_2 = \omega_v (R - d_\omega / 2 \end{cases} \tag{16}$$

$$\begin{aligned} \omega_{mr}^* &= \frac{L_\omega - (d_\omega / 2)\tan(\delta)}{L_\omega} \omega_{mr} \\ \omega_{ml}^* &= \frac{L_\omega - (d_\omega / 2)\tan(\delta)}{L_\omega} \omega_{ml} \end{aligned} \tag{17}$$

Where ω_v is the vehicle angular speed according to the center of turn.

The difference between wheel drive angular speeds is then:

$$\Delta\omega = \omega_{mr}^* - \omega_{ml}^* = -\frac{d_\omega \tan(\delta)}{L_\omega} \omega_v \tag{18}$$

And the steering angle indicates the trajectory direction:

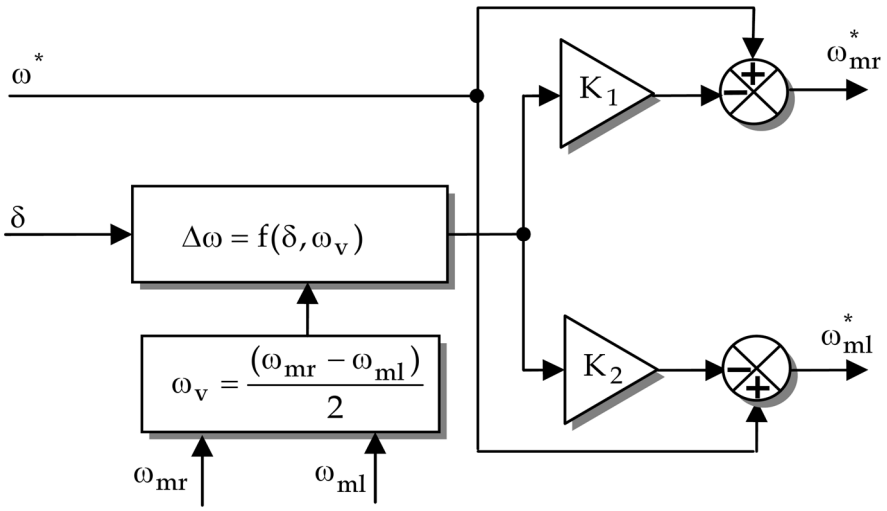

Fig. 11. Differential electronic.

$$\delta > 0 \Rightarrow Turn\,left \tag{19}$$

$$\delta = 0 \Rightarrow Straight\,ahead$$

$$\delta < 0 \Rightarrow Turn\,raight$$

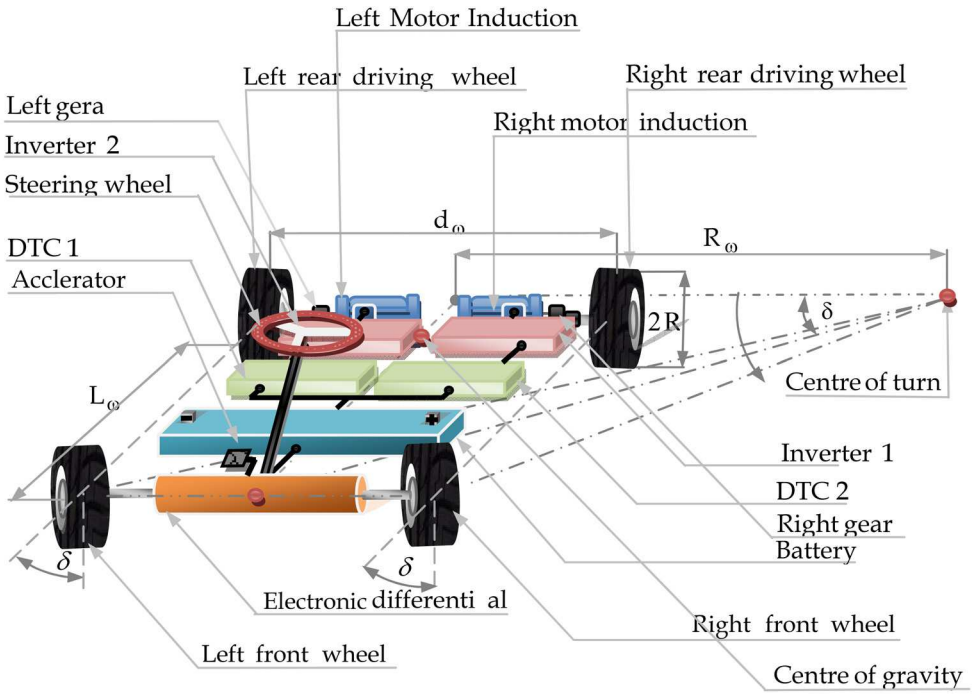

Fig. 12. Structure of vehicle in curve

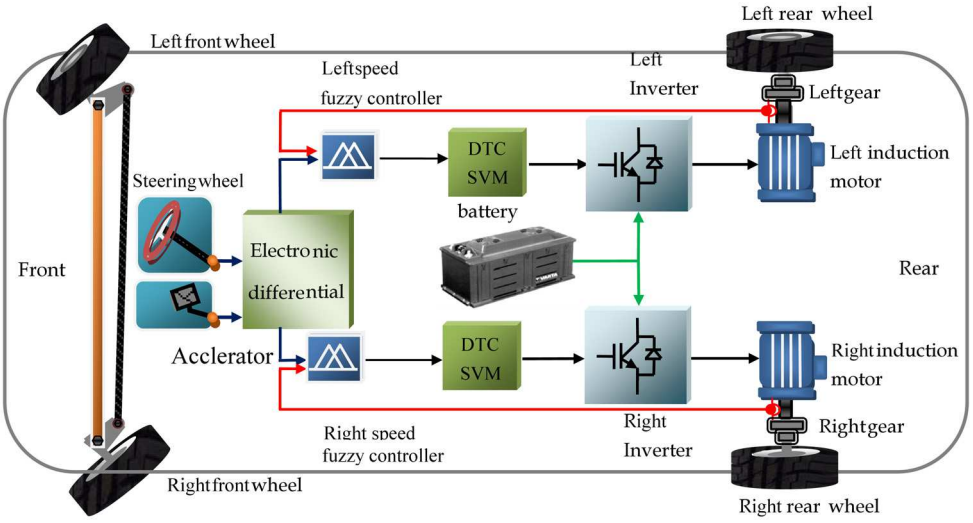

Fig. 13. The riving wheels control system

7. Simulation results

In order to characterize the driving wheel system behavior, Simulations were carried using the model of Fig 13.The following results was simulated in MATLAB .The test demonstrate the EV performances using an intelligence fuzzy PI controlled with DTC-SVM strategy under several speed variation.

A: Intelligent fuzzy PI controller with space vector modulation

The topology studied in this present work consists of three phases: the first one represent the acceleration phase's beginning with 60 Km/h in straight road, the second phase represent the deceleration one when the speed became 30 Km/h, and finally the EV is moving up the slopped road of 10% under 80 Km/h, the specified road topology is shown in Fig. 14, when the speed road constraints are described in the Table 2.

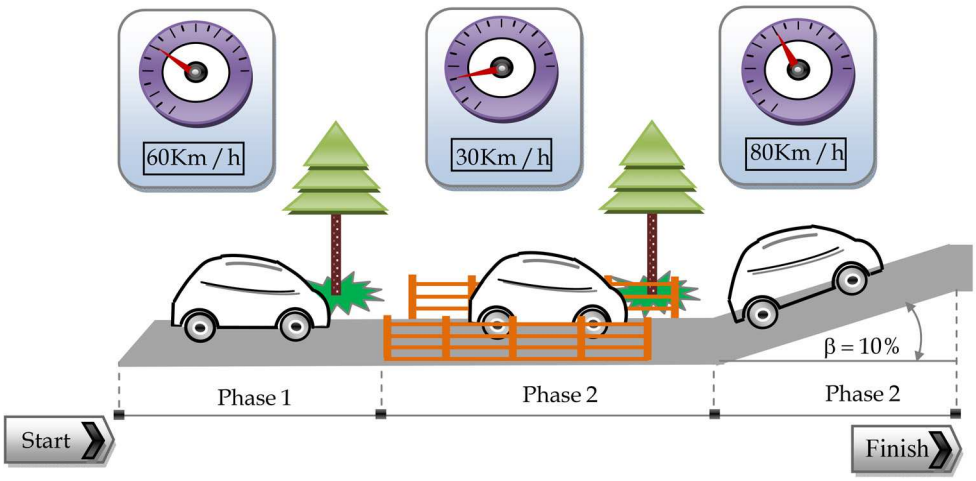

Fig. 14. Specify driving route topology

Phases	Event information	Vehicle Speed [km/h]
Phase 1	Acceleration	60
Phase 2	Bridge, Break	30
Phase 3	Acceleration and climbing a slope 10%	80

Table 3. Specified driving route topology

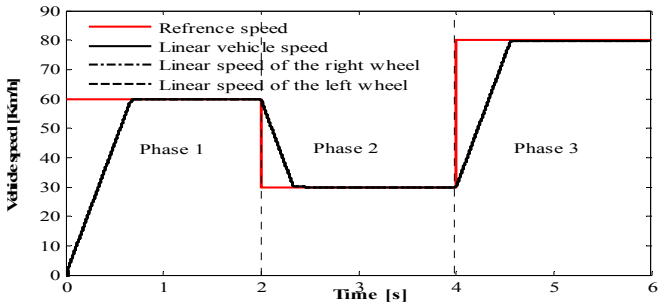

Fig. 15. Variation of vehicle speeds in different phases.

Refereed to Fig. 15 at time of 2 s the vehicle driver move on straight road with linear speed of 60 km/h, the assumption's that the two motors are not disturbed. In this case the driving wheels follow the same path with no overshoot and without error which can be justified with the good electronic differential act coupled with DTC-SVM performances.

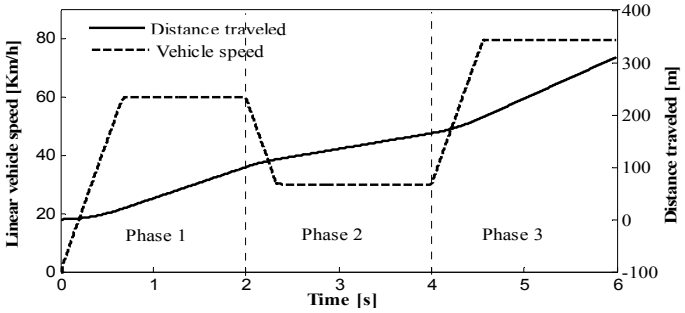

Fig. 16. Evaluation of vehicle and distance travelled in different phases.

Fig. 16, reflect the relationship between vehicle speed's variation and distance traveled in different phases. The distance travelled of 310 m in three electronic differential references acts 60 then break of 30 and acceleration until 80 km/h.

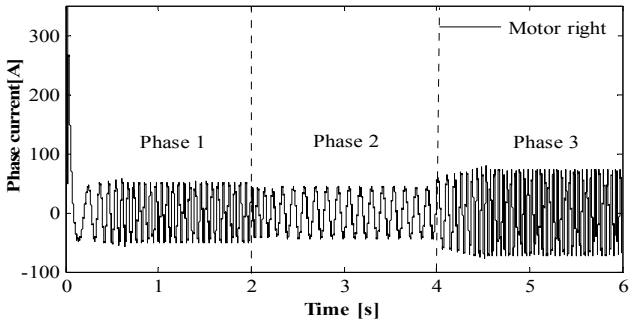

Fig. 17. Variation of phase current of the right motor in different phases.

Figs 17 and 18 explains the variation of phase current and driving force respectively. In the first step and to reach 60 km/h The EV demand a current of 50.70 A for each motor which explained with driving force of 329.30N. In second phase the current and driving forces demand decrees by means that the vehicle is in recharging phase's which explained with the decreasing of current demand and developed driving forces shown in Figs 14 and 15 respectively . The last phases explain the effect of acceleration under the slope on the straight road EV moving. The driving wheels forces increase and the current demand undergo double of the current braking phases the battery use the maximum of his power to satisfy the motorization demand under the slopped road condition which can interpreted physically the augmentation of the globally vehicle resistive torque illustrate in Table 4. In the other hand the linear speeds of the two induction motors stay the same and the road drop does not influence the torque control of each wheels. The results are listed in Table 3.

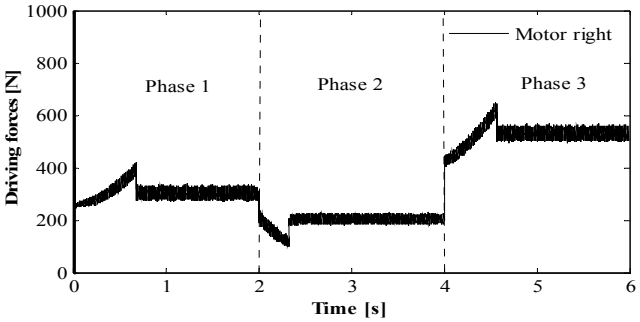

Fig. 18. Variation of driving force of the right motor in different phases.

Phases	1	2	3
the Vehicle resistive torque [N.m]	95.31	68.53	168.00
the globally vehicle resistive torque Percent compared with nominal motor torque of 476 Nm	20.02 %	14.39 %	35.29 %

Table 4. Variation of vehicle torque in different Phases.

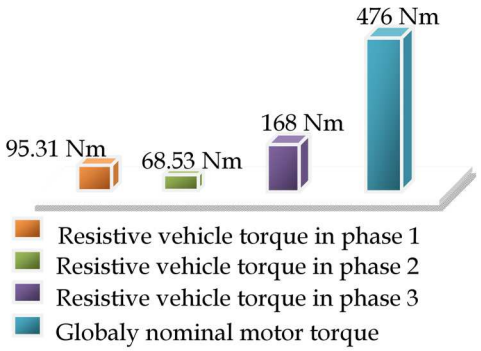

Fig. 19. Evaluation of the globally vehicle resistive torque compared to nominal motor torque in different phases.

According to the formulas (2),(3),(4) and Table. 3, the variation of resistive vehicle torques in different cases as depicted in Table 4. , the vehicle resistive torque was 95.31 N.m in the first case (acceleration phase) when the power propulsion system resistive one is only 68.53 Nm in the breaking phases (phases 2) , the back driving wheels develop more and more efforts to satisfy the traction chain demand which impose an resistive torque equal to 168.00 N.m .The result prove that the traction chain under acceleration demand develop the double effort comparing with the breaking phase case's by means that the vehicle needs the half of its energy in the deceleration phase's compared with the acceleration one's as it specified in table 2.

B. Comparative study of two method of controlling

In simulations the two different methods to control the EV were used .Because of the sweeping of the kp on the interval [15 43] and the ki on the interval [228 243] as shown in the figure 20 and 21.The DTC with Fuzzy Adaptive PI Control method improves EV performance. The intelligent fuzzy PI controller was proved in efficiency adaptation for stability of the vehicle. The results obtained by simulation show that this structure permits the realization of the robust control based on intelligent fuzzy inference system, with good dynamic and static performances for the multi-converters/multi-machines propelled system.

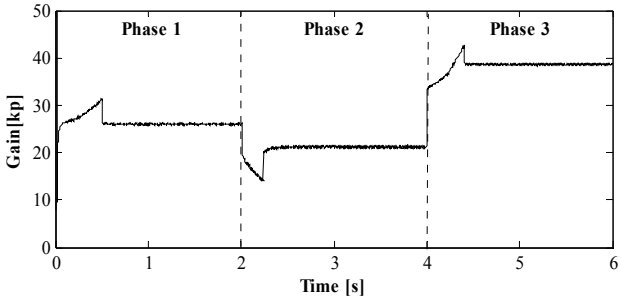

Fig. 20. Variation gain kp of intelligent fuzzy PI controller

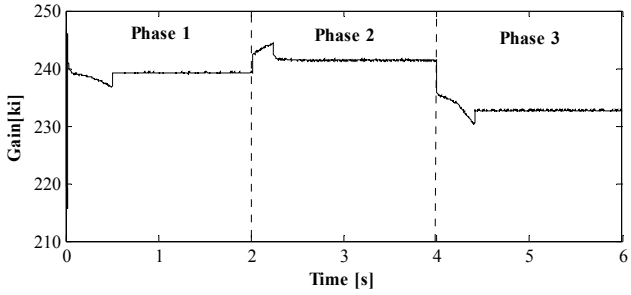

Fig. 21. Varaition gain ki of adaptive fuzzy PI controller

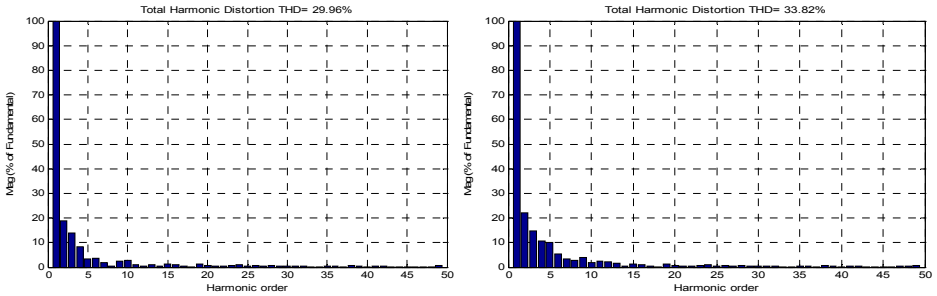

(a) (b)

Fig. 22. (a) Total harmonic distortion using DTC with intelligent fuzzy PI controller, (b) Total harmonic distortion using DTC-SVM with classical PI.

Referring to figures 20 (a) and (b) we show harmonic analyses of stator current. DTC-SVM with intelligent fuzzy PI controller present 29.96%, DTC-SVM with classical PI controller give 33.82 %. The first controller offer an reduction of 13.84% .This remarkable change obtained enables us to say that the current inject by voltage source inverter in DTC-SVM classical PI controller is harmonics current polluting what to justify the great oscillations of the torque and the attraction force .as a consequence this ripple present negative effects on the autonomy of the battery and heating of the both motors and increase power losses.

Designation	PI controller	intelligent fuzzy PI controller
THD [%]	33.82	29.96
Comportment of electric vehicle in sloped road	Less adaptive	More adaptive
Driving forces and electromagnetic torque	More oscillation	Less oscillation

Table 5. Comparative between PI and intelligent fuzzy PI controller

8. Conclusions

The research outlined in this paper has demonstrated the feasibility of an improved vehicle stability which utilizes two independent back drive wheels for motion by using DTC-SVM controls. DTC-SVM with intelligent Fuzzy control is able to adapt itself the suitable control parameters which are the proportional and integral gains kp and ki to the variations of vehicle torque. This method was Improved EV steering and stability during different trajectory. The advantage DTC-SVM controller is robustness and performance, there capacity to maintain ideal trajectories for two wheels control independently and ensure good disturbances rejections with no overshoot and stability of vehicle perfected ensured with the speed variation and less error speed. The DTC-SVM with intelligent fuzzy PI controller is more adaptive for propelled systems. The electric vehicle was proved best comportment and stability during different road path by

maintaining the motorization error speed equal zeros and gives a good distribution for deriving forces. The electric vehicle was proved efficiency comportment in the different road constraints.

Te	Motor traction torque	238 Nm
Je	Moment on inertia of the drive train	7.07Kgm2
Rw	Wheel radius	0.32m
M	Vehicle mass	1300Kg
fe	Bearing friction coefficient	0.32
Kd	Aerodynamic coefficient	0.32
A	Vehicle frontal area	2.60 m2
fv	Vehicle friction coefficient	0.01
Lw	Distance between two wheels and axes	2.5m
dw	Distance between the back and the front wheel	1.5m

Table 6. Vehicle Parameters.

9. References

[1] Yee-Pien Yang., Chun-Pin Lo. Current Distribution Control of Dual Directly Driven Wheel Motors for Electric Vehicles, *Control Engineering Practice, vol.* 16, no. 11, pp. 1285-1292, 2008.

[2] P. He., Y. Hori., M. Kamachi ., K. Walters., H. Yoshida. Future Motion Control to be Realized by In-wheel Motored Electric Vehicle, *In Proceedings of the 31st Annual Confer- ence of the IEE Industrial Electronics Society, IEEE Press, Raliegh South Carolina,* USA, pp. 2632-2637, 2005.

[3] Jun-Koo Kang ., Seung-Ki Sul. New Direct Torque Control of Induction Motor for Minimum Torque Ripple and Constant Switching Frequency, *IEEE Trans. Ind. Applicat., vol*. 35, no. 5, p. 1076-1082, 1999.

[4] C. C. Chan . Electric vehicles charge forward*, IEEE Power Energy Mag, vol*. 2, no. 6, pp. 24–33, 2004.

[5] Z. Q. Zhu ., David HoweZ. Zhu . Electrical machines and drives for electric, hybrid, and fuel cell vehicles, *Proc. IEEE, vol. 95, no. 4,* pp. 764–765, 2007.

[6] P. Vas. Sensorless Vector and Direct Torque Control, *Oxford University Press*, 1998.

[7] K. Itoh ., H. Kubota. Thrust ripple reduction of linear induction motor with direct torque control, *Proceedings of the Eighth International Conference on Electrical Machines and Systems, ICEMS 2005, vol*. 1, pp. 655-658, 2005.

[8] Lin Chen j, Kang-Ling Fang chen . A Novel Direct Torque Control for Dual-Three-Phase Induction Motor, *Conf. Rec. IEEE International Conference on Machine Learning and Cybernetics,* pp. 876-88, 2003.

[9] P. Vas. Sensorless Vector and Direct Torque Control, Oxford University Press, 1998.

[10] [10] A. Schell., H. Peng., D. Tran., E.Stamos. Modeling and Control Strategy development for Fuel Cell Electric Vehicle, *Annual Review in control Elseiver, vol*. 29, pp. 159-168, 2005.

[11] A. Haddoun., M. Benbouzid., D. Diallo., R. Abdesseme.,, J. Ghouili., K. Srairi. Modeling ,Analysis and neural network control of an EV Electrical Differentiel, *Transaction on industriel electronic vol*. 55,N 6 June 2008.

[12] A. Nasri., A .Hazzab .,I.K. Bousserhane., S. Hadjeri., P. Sicard., Two Wheel Speed Robust Sliding Mode Control For Electric Vehicle Drive, Serbian Journal of Electrical Engineering , vol. 5, no.2, pp. 199-216, 2008.

[13] K. Hartani., M.bourahla,. Y.miloud, M.sekour., Electronic Differential with Direct Torque Fuzzy Control for Vehicle Propulsion System, Turk J Elec Eng & Comp Sci, vol.17, no.1, 2009, TUBITAK.

[14] L.T. Lam., R. louey. Developpement of ultra-battery for hybrid-electric vehicle applications, *Elservier, power sources, vol*. 158, pp. 1140-1148, 2006.

[15] Larminie. Electric Vehicle Technology Explained, *Edited by John Wiley and John Lowry, England*, 2003.

[16] A. Haddoun et al. Analysis, modeling and neural network traction control of an electric vehicle without differential gears, *in Proc. IEEE IEMDC, Antalya, Turkey, May* 2007, pp. 854–859.

[17] M. Vasudevan., R. Arumugam ., New direct torque control scheme of induction motor for electric vehicles, 5th Asian Control Conference, vol. 2, pp. 1377 – 1383, 2004.

[18] M. E. H. Benbouzid et al. Advanced fault-tolerant control of inductionmotor drives for EV/HEV traction applications, *From conventional to modern and intelligent control techniques, IEEE Trans. Veh. Technol., vol.* 56, no. 2, pp. 519–528, Mar. 2007.

[19] A. Gupta., A. M. Khambadkone. A space vector pwm scheme for multilevel inverters based on two-level space vector pwm, *IEEE Transaction on Industrial Electronics, vol.* 53, October 2006.

[20] T. G. Habetler., F. Profumo., M.Pastorelli., L. Tolbert. Direct torque control of induction machines using space vector modulation*, IEEE Transaction on Industry Applications, vol.* 28, no. 5, pp. 1045-1053, septembre/October 1992.

[21] Mingqian Gao., Shanghong He. Self-adapting Fuzzy-PID Control of Variable Universe in the Non-linear System, *2008 International Conference on Intelligent Computation Technology and Automation*.

[22] J.-Y. Chen, P.-S. Tsai and C.-C. Wong .Adaptive design of a fuzzy cerebellar model arithmetic controller neural network, *IEE Proc.-Control Theory and pplications, vol.* 152, no.2, pp. 133-137, 2005.

[23] Chih-Min Lin., Ya-Fu Peng., Adaptive CMAC-Based Supervisory Control for Uncertain Nonlinear Systems, IEEE Transactions on systems, man, and cybernetics-part b: cybernetics, vol. 34, no. 2, april 2004.

[24] Hugang Han., Chun-Yi Su., Yury Stepanenko. Adaptive control of a class of nonlinear systems with nonlinearly parameterized fuzzy approximators, *IEEE transactions on fuzzy systems, vol*. 9, no. 2, april 2001.

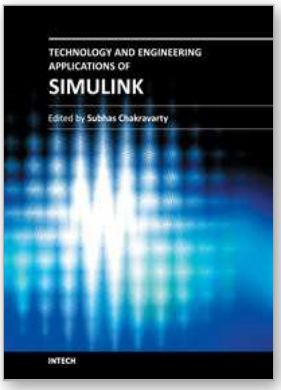

Technology and Engineering Applications of Simulink

Edited by Prof. Subhas Chakravarty

ISBN 978-953-51-0635-7
Hard cover, 256 pages
Publisher InTech
Published online 23, May, 2012
Published in print edition May, 2012

Building on MATLAB (the language of technical computing), Simulink provides a platform for engineers to plan, model, design, simulate, test and implement complex electromechanical, dynamic control, signal processing and communication systems. Simulink-Matlab combination is very useful for developing algorithms, GUI assisted creation of block diagrams and realisation of interactive simulation based designs. The eleven chapters of the book demonstrate the power and capabilities of Simulink to solve engineering problems with varied degree of complexity in the virtual environment.

How to reference

In order to correctly reference this scholarly work, feel free to copy and paste the following:

Brahim Gasbaoui and Abdelfatah Nasri (2012). The Uses of Artificial Intelligence for Electric Vehicle Control Applications, Technology and Engineering Applications of Simulink, Prof. Subhas Chakravarty (Ed.), ISBN: 978-953-51-0635-7, InTech, Available from: http://www.intechopen.com/books/technology-and-engineering-applications-of-simulink/the-uses-of-artificial-intelligence-for-electric-vehicle-control-applications

INTECH
open science | open minds

InTech Europe
University Campus STeP Ri
Slavka Krautzeka 83/A
51000 Rijeka, Croatia
Phone: +385 (51) 770 447
Fax: +385 (51) 686 166
www.intechopen.com

InTech China
Unit 405, Office Block, Hotel Equatorial Shanghai
No.65, Yan An Road (West), Shanghai, 200040, China
中国上海市延安西路65号上海国际贵都大饭店办公楼405单元
Phone: +86-21-62489820
Fax: +86-21-62489821